

# An External $\delta$ -Carbonic Anhydrase in a Free-Living Marine Dinoflagellate May Circumvent Diffusion-Limited Carbon Acquisition<sup>1[W]</sup>

Mathieu Lapointe<sup>2,3</sup>, Tyler D.B. MacKenzie<sup>2,4</sup>, and David Morse\*

Institut de Recherche en Biologie Végétale, Département de Sciences Biologiques, Université de Montréal, Montreal, Quebec, Canada H1X 2B2

The oceans globally constitute an important sink for carbon dioxide (CO<sub>2</sub>) due to phytoplankton photosynthesis. However, the marine environment imposes serious restraints to carbon fixation. First, the equilibrium between CO<sub>2</sub> and bicarbonate (HCO<sub>3</sub><sup>-</sup>) is pH dependent, and, in normal, slightly alkaline seawater, [CO<sub>2</sub>] is typically low (approximately 10  $\mu$ M). Second, the rate of CO<sub>2</sub> diffusion in seawater is slow, so, for any cells unable to take up bicarbonate efficiently, photosynthesis could become carbon limited due to depletion of CO<sub>2</sub> from their immediate vicinity. This may be especially problematic for those dinoflagellates using a form II Rubisco because this form is less oxygen tolerant than the usually found form I enzyme. We have identified a carbonic anhydrase (CA) from the free-living marine dinoflagellate *Lingulodinium polyedrum* that appears to play a role in carbon acquisition. This CA shares 60% sequence identity with  $\delta$ -class CAs, isoforms so far found only in marine algae. Immunoelectron microscopy indicates that this enzyme is associated exclusively with the plasma membrane. Furthermore, this enzyme appears to be exposed to the external medium as determined by whole-cell CA assays and vectorial labeling of cell surface proteins with <sup>125</sup>I. The fixation of <sup>14</sup>CO<sub>2</sub> is strongly pH dependent, suggesting preferential uptake of CO<sub>2</sub> rather than HCO<sub>3</sub><sup>-</sup>, and photosynthetic rates decrease in the presence of 1 mM acetazolamide, a non-membrane-permeable CA inhibitor. This constitutes the first CA identified in the dinoflagellates, and, taken together, our results suggest that this enzyme may help to increase CO<sub>2</sub> availability at the cell surface.

Oceanic phytoplankton contribute roughly one-half of the total global photosynthetic carbon fixation (Behrenfeld et al., 2006), despite the fact that availability of dissolved CO<sub>2</sub> (the direct substrate of Rubisco) in the marine environment is generally low (approximately 10  $\mu$ M). Indeed, most of the dissolved inorganic carbon (DIC) in the ocean is bicarbonate (approximately 2 mM HCO<sub>3</sub><sup>-</sup>), and thus phytoplankton have had to develop a panoply of mechanisms to cope with the critical step of acquiring carbon from the environment (Giordano et al., 2005). The situation is particularly difficult for phytoplankton that lack the capacity to transport HCO<sub>3</sub><sup>-</sup> because dehydration of HCO<sub>3</sub><sup>-</sup> to CO<sub>2</sub> is generally considered to be slow (uncatalyzed half-life approximately 1 min) and the diffusion of CO<sub>2</sub> in aqueous solution is much slower than in air. Rapid

photosynthesis by these phytoplankton can potentially remove CO<sub>2</sub> from their immediate surroundings faster than it can be replenished, potentially limiting carbon fixation by carbon availability (Riebesell et al., 1993).

Dinoflagellates are a major constituent of the oceanic phytoplankton and, unlike all other eukaryotic phytoplankton, use a form II Rubisco as their primary carbon-fixing enzyme (Morse et al., 1995). Dinoflagellate form II Rubisco has a lower affinity and lower CO<sub>2</sub>/O<sub>2</sub> specificity than the more common form I Rubisco (Whitney and Andrews, 1998), suggesting net carbon fixation in dinoflagellates should be unfavorable at the low ambient CO<sub>2</sub> levels in the marine environment. This indicates these cells probably have sophisticated biophysical mechanisms to increase CO<sub>2</sub> concentration within the cell to assure an adequate carbon supply (Giordano et al., 2005).

The enzyme carbonic anhydrase (CA; EC 4.2.1.1), which mediates the rapid interconversion of CO<sub>2</sub> and HCO<sub>3</sub><sup>-</sup>, is an important part of most mechanisms used to alleviate the restriction of CO<sub>2</sub> near Rubisco in marine phytoplankton. Most directly, CA within the chloroplast would act to maintain the equilibrium concentration of CO<sub>2</sub> at stromal pH and thus provide a source of CO<sub>2</sub> formation in the vicinity of Rubisco (Jacobson et al., 1975). Alternatively, many algae have developed some form of a CO<sub>2</sub>-concentrating mechanism (CCM) to transport inorganic carbon into the cell (Giordano et al., 2005). CCMs can take many forms, but often include CA to increase the rate of intercon-

<sup>1</sup> This work was supported by the National Science and Engineering Research Council (NSERC) of Canada (grant no. 171382-03). T.D.B.M. was the beneficiary of an NSERC postdoctoral fellowship.

<sup>2</sup> These authors contributed equally to the article.

<sup>3</sup> Present address: Département de Biologie Cellulaire, Université de Montréal, Montreal, Quebec, Canada H1X 2B2.

<sup>4</sup> Present address: Monroe Community College, Rochester, NY 14623.

\* Corresponding author; e-mail david.morse@umontreal.ca.

The author responsible for distribution of materials integral to the findings presented in this article in accordance with the policy described in the Instructions for Authors ([www.plantphysiol.org](http://www.plantphysiol.org)) is: David Morse ([david.morse@umontreal.ca](mailto:david.morse@umontreal.ca)).

<sup>[W]</sup> The online version of this article contains Web-only data.

[www.plantphysiol.org/cgi/doi/10.1104/pp.108.117077](http://www.plantphysiol.org/cgi/doi/10.1104/pp.108.117077)

version of  $\text{CO}_2$  and  $\text{HCO}_3^-$  in different intra- and extracellular spaces. For example,  $\text{HCO}_3^-$  transported into the acidic thylakoid lumen could be efficiently transformed by a luminal CA to  $\text{CO}_2$ , which could then diffuse freely out into the stroma (Raven, 1997). In addition, intracellular CAs could trap  $\text{CO}_2$  within compartments by converting it into membrane-impermeable  $\text{HCO}_3^-$  (Rumeau et al., 1996). Last, an extracellular CA (eCA) located on the outer surface of the plasma membrane could accelerate the conversion of the abundant  $\text{HCO}_3^-$  in seawater, in the immediate vicinity of the cell, to  $\text{CO}_2$ , which could freely diffuse into the cell. CA activity is so important for carbon metabolism that most algae likely employ several different CA isoforms acting in concert to ensure an adequate supply of  $\text{CO}_2$  to Rubisco (Sültemeyer, 1998).

CA activity is distributed in phytoplankton (Moroney et al., 2001) and has been found within all studied species of dinoflagellates, including symbiotic species (Leggat et al., 2002) and those species free living in marine (Nimer et al., 1997, 1999; Leggat et al., 1999; Dason et al., 2004; Rost et al., 2006; Ratti et al., 2007) or freshwater (Berman-Frank et al., 1994, 1995) environments. eCA activity is less common, but has been reported in several species of phytoplankton from diverse groups, including some species of dinoflagellates (Berman-Frank et al., 1995; Nimer et al., 1997, 1999). These eCA activities are generally observed only under carbon-limited conditions, although it has been reported that several marine dinoflagellates displaying eCA activity when carbon limited also had a low constitutive eCA activity in carbon-replete conditions (Nimer et al., 1997). The requirement for this constitutive eCA was ascribed to the presence of form II Rubisco.

All CA enzymes have remarkably high catalytic rates and are able to greatly accelerate the interconversion of  $\text{HCO}_3^-$  ions and  $\text{CO}_2$ . There are four main, yet evolutionarily unrelated, families of CA ( $\alpha$ -,  $\beta$ -,  $\gamma$ -,  $\delta$ -types) distributed among bacteria, animals, and plants (Tripp et al., 2001). All are obligate metalloenzymes because removal of the normally bound  $\text{Zn}^{2+}$  by dialysis leads to inactivity. Interestingly, the  $\delta$ -CA has so far been reported only in marine algae (Roberts et al., 1997; Tripp et al., 2001; Soto et al., 2006). A new family, termed  $\zeta$ -CA, has recently been described that binds  $\text{Cd}^{2+}$  instead of  $\text{Zn}^{2+}$  (Lane et al., 2005) and also lacks sequence homology to other CA types. This latter isoform has also been documented in cyanobacteria (So et al., 2004).

We report here the identification and characterization of a dinoflagellate  $\delta$ -CA. This enzyme is located on the external face of the plasma membrane and CA activity in whole cells is susceptible to the poorly membrane-permeable CA inhibitor acetazolamide (AZ). Carbon fixation rates are also sensitive to AZ, suggesting that the  $\delta$ -CA may generate membrane-permeable  $\text{CO}_2$  from the more abundant  $\text{HCO}_3^-$  at the cell periphery to support an increased photosynthetic rate. This constitutes the first CA identified from the dinoflagellates.

## RESULTS

### *Lingulodinium* Expresses a $\delta$ -CA Isoform

Two different CA cDNA sequences (LpCA1 [1.03 kb] and LpCA2 [1.18 kb]) were isolated from a *Lingulodinium polyedrum* cDNA library by colony hybridization using a PCR product with sequence homology to a  $\delta$ -CA from the diatom *Thalassiosira weissflogii* (TWCA1). Western blot performed with an antibody raised against TWCA1 (Roberts et al., 1997) and affinity purified against the LpCA2 expressed in bacteria showed only a single band of 31 kD in extracts from *Lingulodinium* (Fig. 1A, lane 1). Because the LpCA2 sequence detects a polyadenylated RNA of roughly 1,600 nucleotides in *Lingulodinium* RNA (Fig. 1B), the original clones were not complete. To attempt to recover the remaining 5' sequence, we performed nested PCR using internal sequences from either LpCA1 or LpCA2 cDNA and the 5' trans-sliced leader common to all dinoflagellate mRNA (Zhang et al., 2007). Although this procedure was not successful for LpCA1, the complete 5' end was recovered for LpCA2. The LpCA1 and LpCA2 shared 80% amino acid sequence identity in the region of overlap and between 58% and 62% amino acid sequence identity with TWCA1 (Supplemental Fig. S1).

Both LpCA1 and LpCA2 have homologs with incomplete sequences in EST banks derived from the dinoflagellates *Karlodinium micrum*, *Karenia brevis*, *Alexandrium tamarense*, and *L. polyedrum*. Interestingly, no sequences were recovered from the dinoflagellate *Amphidinium carterae*, in agreement with the observation that no  $\delta$ -CA was detected in extracts from *A. carterae* using the affinity-purified antibody (Fig. 1A, lane 2). An

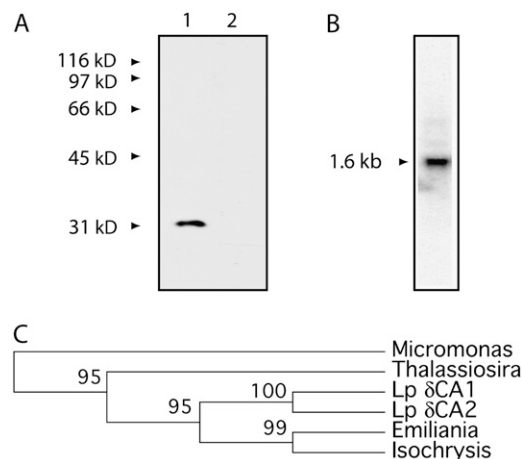


**Figure 1.** *Lingulodinium* expresses a  $\delta$ -CA similar to that of haptophytes. A, Affinity-purified antibody raised against *Thalassiosira*  $\delta$ -CA reacts with a 31-kD protein from *Lingulodinium* on western-blot analysis. B, The *Lingulodinium*  $\delta$ -CA is expressed as a roughly 1.6-kb RNA by northern-blot analysis. C, Phylogenetic analysis places the two *Lingulodinium*  $\delta$ -CAs close to those of haptophytes (*Emiliana huxleyi* and *Isochrysis galbana*) and stramenopiles (*T. weissflogii*) and further from that of a green alga (*Micromonas* sp.).



protocols were tested. We found that extraction of the labeled cell wall fraction using 2% SDS revealed several additional radiolabeled proteins, including one comigrating with the anti- $\delta$ -CA signal (Fig. 3A). The same protein sample, prepared for two-dimensional PAGE (2D-PAGE) by a  $\text{CHCl}_3$ -methanol precipitation, also showed comigration of a radiolabeled protein for each of the four  $\delta$ -CA isoforms resolved by 2D electrophoresis (Fig. 3B). The relative staining intensity between the four different CA isoforms detected by the antibody differs when compared to the radiolabel incorporation, presumably due to the distribution of Tyr residues available for iodination on each protein. Clearly, the  $\delta$ -CA on the cell surface is exposed to the external environment, although these results cannot distinguish between LpCA1 and LpCA2.

To test the possibility that the active site of the  $\delta$ -CA was exposed to the external medium, the amount of immunoreactive protein was compared with intact cell CA activities for cultures grown at two different pHs. Algae grown at alkaline pH often have increased external CA activity, presumably due to a decrease in the ambient  $[\text{CO}_2]$  (Williams and Colman, 1996; Elzenga et al., 2000), and this is also the case for *Lingulodinium* (Fig. 3D, gray bars). When the amount of immunoreactive  $\delta$ -CA was measured by western blots (Fig. 3, C and D, white bars), *Lingulodinium* grown at pH 9 was found to contain twice the immunoreactive  $\delta$ -CA than cells grown at pH 8.2. The increase in intact cell activity is again not due to differential cell breakage because both samples show  $<1\%$  broken cells.

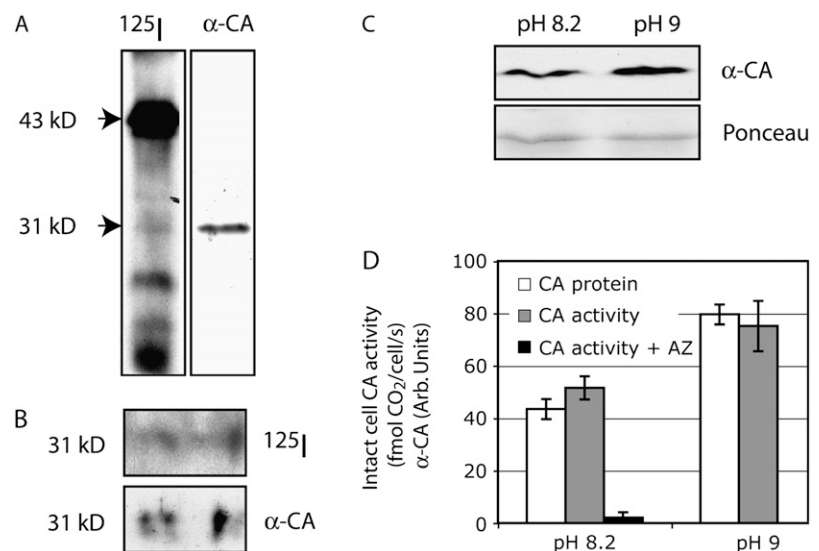
The non-membrane-permeable CA inhibitor AZ (Moroney et al., 1985; Colman et al., 2002) is often used to test for the presence of an external CA. We thus anticipated, based on the exposure of the  $\delta$ -CA to the external medium, that AZ might inhibit CA activity in intact cells. Indeed, AZ greatly reduced the CA activity in intact cells (Fig. 3D, black bar).

### External CA Activity Is Required for Efficient $\text{CO}_2$ Acquisition at $[\text{CO}_2]$ Near the $K_m$

Cells that take up  $\text{CO}_2$  from their environment would be predicted to exploit an external CA to increase carbon acquisition by accelerating the formation of  $\text{CO}_2$  from  $\text{HCO}_3^-$  in the surrounding seawater, thereby regenerating external  $[\text{CO}_2]$  as it is used by the photosynthetic machinery. To discriminate between  $\text{HCO}_3^-$  and  $\text{CO}_2$  uptake, whole-cell photosynthetic carbon fixation rates were measured as a function of the pH, which alters the equilibrium concentrations of the  $\text{HCO}_3^-$  and  $\text{CO}_2$  components of DIC (Schulz et al., 2006). At typical seawater pH,  $\text{HCO}_3^-$  is the most abundant component of DIC and the  $[\text{CO}_2]$  is relatively low; the  $[\text{CO}_2]$  increases markedly as the pH decreases. Our assays, which consist of 30-min incubations in different pH buffers, expose the cells to a dramatic range of  $[\text{CO}_2]$  without appreciable change in the relatively large  $[\text{HCO}_3^-]$ . The equilibrium to a new  $[\text{CO}_2]$  when cell cultures are added to concentrated buffer at the desired pH is expected to occur on a time scale of tens of seconds (Zeebe et al., 1999; Schulz et al., 2006).

In algae, which preferentially use  $\text{CO}_2$  for carbon uptake (Elzenga et al., 2000), photosynthetic activity is expected to decrease at the low  $[\text{CO}_2]$  found at alkaline pH; extrapolation to zero  $[\text{CO}_2]$  should show very low carbon fixation rates. To test this for *Lingulodinium*, an initial series of assays was performed using centrifugation both to concentrate cell cultures roughly 10-fold and to replace the culture medium with buffer containing known concentrations of DIC. By using a range of DIC concentrations at three different pHs, cells were exposed not only to ranges of  $[\text{HCO}_3^-]$  and pH, but also to a wide range in  $[\text{CO}_2]$ , which was determined from the combinations of DIC and pH. This approach thus allows effects of DIC and pH from effects of  $[\text{CO}_2]$

**Figure 3.** Lp- $\delta$ -CA is exposed to the external medium. Vectorial labeling of whole cells with  $^{125}\text{I}$  shows comigration of radiolabel and immunoreactivity with an antibody raised against  $\delta$ -CA ( $\alpha$ -CA) after either SDS-PAGE (A) or 2D-PAGE (B). C, Alkaline pH induces an increased level of signal with the  $\alpha$ -CA as measured by western blot. D, Comparison of immunoreactive protein measurements (as in C) with intact cell CA activity measurements. Means and SD of quadruplicate samples are shown. Treatment of intact cells with the membrane-impermeable CA inhibitor AZ reduces CA activity at both pH levels.



on photosynthetic rate to be distinguished. At each DIC concentration, carbon fixation rates were indeed lower at alkaline pH (Fig. 4A). More importantly, when  $[\text{CO}_2]$  is calculated for each experimental condition and the data replotted on an axis of  $[\text{CO}_2]$ , we observed that the photosynthetic rate tends toward zero when  $[\text{CO}_2]$  approaches zero (Fig. 4B), despite the large reservoir of DIC in the form of  $\text{HCO}_3^-$ . This suggests that  $\text{CO}_2$  is the preferred substrate for carbon fixation. In addition, we observed that carbon fixation rates using different combinations of pH and DIC only follow a single curve when plotted against calculated  $[\text{CO}_2]$ , indicating that  $[\text{CO}_2]$  rather than DIC or pH alone constrains carbon fixation rates and that the kinetic parameters of carbon fixation are unlikely to be affected by pH independent from the known effect of pH on  $[\text{CO}_2]$ .

In assays using centrifuged cells, however, the cells rapidly fall to the bottom of the microtiter plate wells, raising the concern that carbon acquisition by the cells might be reduced by an unusual crowding of the cells and a resulting decrease in cell surface area exposed to

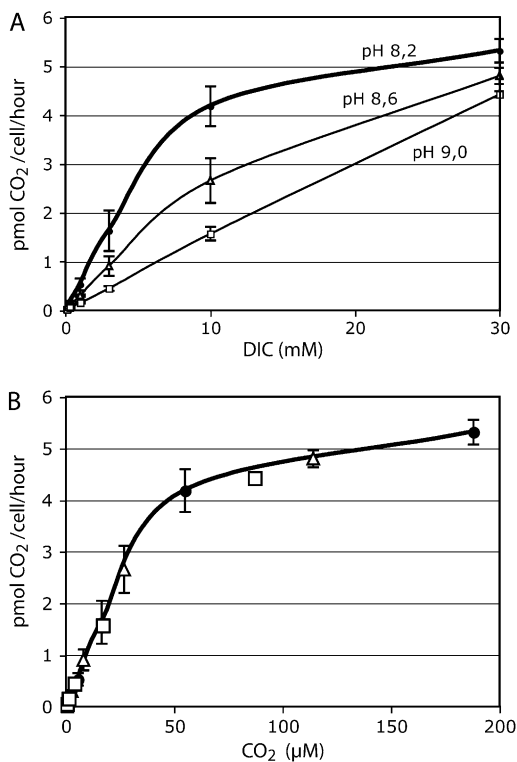


**Figure 4.** *Lingulodinium* preferentially uses  $\text{CO}_2$  for carbon fixation. Carbon fixation rates of *Lingulodinium* cultures concentrated by centrifugation and resuspended in artificial seawater containing different DIC concentrations at three different pH values (black circles, pH 8.3; white triangles, pH 8.7; white squares, pH 9.1). Data are plotted as a function of either DIC concentration (A) or the  $\text{CO}_2$  concentration calculated from Equation 2 (B). The measured pH of the medium containing high  $[\text{HCO}_3^-]$  was used for calculation of  $[\text{CO}_2]$  to correct for the buffering action of  $\text{HCO}_3^-$ .

the medium. This potential problem would be exacerbated by the use of cells concentrated far beyond their normal culture conditions, which could potentially remove  $\text{CO}_2$  from their surroundings more rapidly. To most accurately model  $[\text{CO}_2]$  near the cell and the effect of inhibiting eCA, we therefore decided to measure carbon fixation rates using larger volumes of uncentrifuged cells (i.e. in the original culture medium). While this does not allow replacement of the medium or manipulation of  $[\text{DIC}]$ , because the cells are still swimming, they are surrounded on all sides by the culture medium without crowding, in conditions very similar to their larger parent cultures. These samples recapitulate the essential features observed with centrifuged cells, although, as predicted, generally higher per cell photosynthetic rates are observed consistent with potentially higher  $\text{CO}_2$  availability (Fig. 5A). Again, when  $[\text{CO}_2]$  is calculated for each pH and the data replotted, saturation with  $\text{CO}_2$  and inhibition by AZ can both be observed (Fig. 5B). These curves approximate Michaelis-Menton saturation kinetics and illustrate an increase in the apparent  $K_m$  for  $\text{CO}_2$  in cultures exposed to the CA inhibitor (Fig. 4B). The predicted  $V_{\text{max}}$  is unchanged in the inhibited culture, however, suggesting that sufficiently high  $[\text{CO}_2]$  would still be able to saturate the photosynthetic machinery.

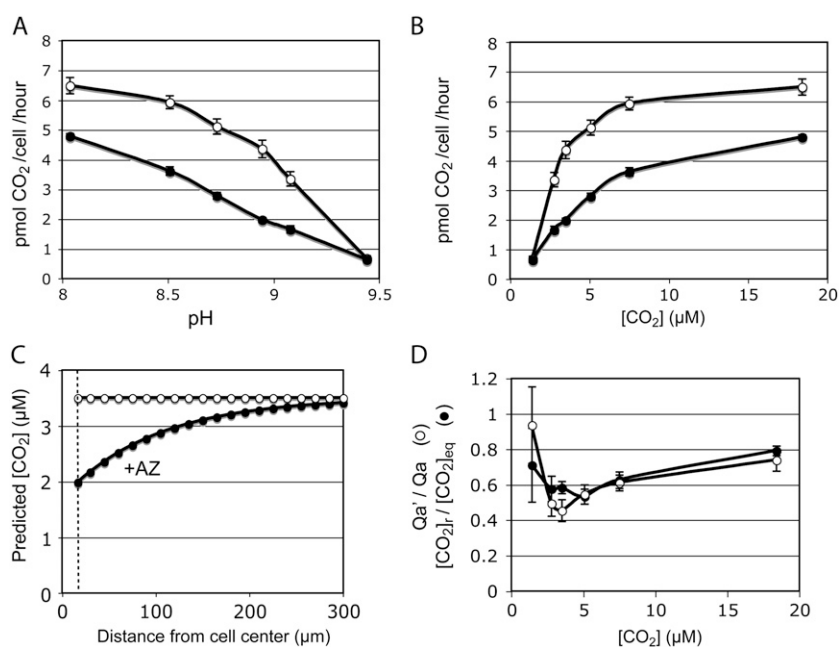
The inhibition of photosynthesis by AZ is consistent with carbon limitation, brought about when photosynthetic rates decrease  $[\text{CO}_2]$  at the cell periphery faster than they can be replenished by diffusion from the bulk medium or the slow uncatalyzed conversion of  $\text{HCO}_3^-$  to  $\text{CO}_2$  near the cell. To test this, we used photosynthetic rates measured in the presence of AZ (black circles) to calculate the  $[\text{CO}_2]$  expected at the cell surface (Fig. 5C, dotted line). As expected, these  $[\text{CO}_2]$  are lower than what would be expected for control cultures able to use an external CA to regenerate equilibrium  $[\text{CO}_2]$  at the cell surface (white circles).

Interestingly, the predicted reduction of  $[\text{CO}_2]$  at the cell surface compared to that in the bulk medium is not constant, but rather is a function of the  $[\text{CO}_2]_{\text{eq}}$  (Fig. 5D, black circles). The predicted reduction in cell surface  $\text{CO}_2$  concentration is less substantial where photosynthesis rates are low (i.e. at low  $[\text{CO}_2]$ ) and where photosynthesis rates are very high (due to saturating  $[\text{CO}_2]$ ), and greatest at intermediate  $[\text{CO}_2]$  more typical of normal growth conditions. These predicted cell surface  $[\text{CO}_2]$  agree well with the degree to which the photosynthetic rate itself is inhibited by AZ (Fig. 5D, white circles).

## DISCUSSION

We report here the identification of a CA in a free-living marine dinoflagellate (Fig. 1A). This enzyme is a  $\delta$ -CA isoform, similar to that expressed in a wide range of marine algae, including chlorophytes, haptophytes, and streptophytes. Despite the limited number

**Figure 5.** External CA activity is required for efficient carbon fixation. A, Carbon fixation rates of *Lingulodinium* cultures in the presence (black circles) or absence (white circles) of 1 mM AZ either as a function of pH (A) or as a function of the  $\text{CO}_2$  concentration (B; calculated from Eq. 2). C,  $\text{CO}_2$  concentrations at various distances from the cell center (black circles) calculated from the photosynthesis rates of an AZ-inhibited culture at pH 8.7 (using Eq. 1). At the cell surface (dotted vertical line), the  $[\text{CO}_2]$  around uninhibited cultures is expected to be identical to that in the bulk medium due to an accelerated interconversion by the external CA. D, Comparison of calculated  $\text{CO}_2$  concentrations at the cell periphery ( $[\text{CO}_2]_r$ ) relative to bulk  $\text{CO}_2$  concentrations (black circles) as well as the photosynthetic rates in AZ-inhibited cultures ( $Q_{a'}$ ) relative to control cultures ( $Q_a$ ; white circles).



of species from which this sequence has been recovered, the mature protein sequence from the dinoflagellates appears more closely related to the haptophytes than to the streptophytes, the phytoplankton expected to be their closest relatives. It is possible that this gene may have arisen in some of the species by lateral gene transfer (Fig. 1C) because a growing number of examples suggest lateral gene transfer of dinoflagellate genes may be relatively frequent (Fagan et al., 1998; Keeling and Inagaki, 2004; Waller et al., 2006). In any event, it is noteworthy that, to date, the  $\delta$ -CA family appears restricted to marine algae.

It also is important to note that the sequence similarity observed with the mature protein sequence does not extend to the N-terminal leader sequence. Unlike the diatom sequence (Roberts et al., 1997), the N terminus of the *Lingulodinium*  $\delta$ -CA contains a predicted signal peptide consistent with secretion of the protein (Fig. 2A). This predicted secretion of the protein is in agreement with the results of vectorial labeling using membrane-impermeable  $^{125}\text{I}$ , confirming that at least part of the  $\delta$ -CA is exposed to the external environment. Furthermore, both immunogold labeling showing an association with the plasma membrane (Fig. 2D) and association of the immunoreactive protein following low-speed subcellular fractionation are both consistent with this interpretation. It is curious that a secreted protein would remain associated with the particulate fraction after cell lysis and fractionation, and this suggests the  $\delta$ -CA may be held at the membrane by association with other proteins or by posttranslational modifications. One possibility for such an anchor may be S-acylation because CSS-Palm predicts the presence of a high-confidence palmitoylation site in the primary sequence.

To address whether the enzyme's active site could be exposed at the external face of the membrane, the

amount of immunoreactive protein was compared with the amount of activity measured in intact cells (Fig. 3C). When cells grown at pH 8.2 were compared with cells grown at pH 9, a similar increase in the amount of immunoreactive protein and the amount of whole cell CA activity is observed. While we cannot exclude the possibility that a different CA, also present at the cell surface, increases in concert with the amount of the  $\delta$ -CA, these results are certainly consistent with the view that the  $\delta$ -CA has an active site on the external face of the cell.

The precise role played by external CA activity in inorganic carbon uptake is still controversial. For example, in *Chlamydomonas reinhardtii*, the inhibition of  $\text{O}_2$  evolution by membrane-impermeable CA inhibitors at alkaline pH (where  $[\text{CO}_2]$  is low) was taken to support a role for the external CA in carbon acquisition (Moroney et al., 1985). However, mutants lacking the major periplasmic CA isoform CAH1 have no phenotype (Van and Spalding, 1999), indicating that this CA is not essential for growth. Possibly, the ability of *C. reinhardtii* to also use  $\text{HCO}_3^-$  (Williams and Turpin, 1987; Spalding, 2008) may contribute to the difficulty is ascribing a role to this external CA.

Interestingly, the *Thalassiosira*  $\delta$ -CA is unlikely to be directed to the plasma membrane, and, although the protein is induced by  $\text{CO}_2$ , there is no direct evidence for an involvement of this enzyme in photosynthesis (Lane and Morel, 2000). The function of the large N-terminal extension (approximately 300 amino acids) of the *Emiliania*  $\delta$ -CA is unknown because its size is more suggestive of a functional domain rather than a targeting signal. The different N-terminal extensions found in the  $\delta$ -CAs of these three species may be a consequence of lateral gene transfer between organisms with subsequent selection of different targeting sequences to fulfill different requirements.

The targeting of a given CA to a particular subcellular location may provide clues to the role played by the enzyme in photosynthesis. For the external  $\delta$ -CA in *L. polyedrum*, this role may involve sustaining the equilibrium concentration of  $\text{CO}_2$  at the cell boundary to compensate for use of  $\text{CO}_2$  in photosynthesis. This can be directly observed by the reduction in carbon fixation rates following addition of the poorly membrane-permeable CA inhibitor AZ (Fig. 5A). The simplest interpretation of this inhibition is that when the observed photosynthesis rates exceed the capacity of diffusion to restore the  $[\text{CO}_2]$  at the cell surface to equilibrium concentrations, the cells become carbon limited and the rate of carbon fixation decreases. There are several caveats to this interpretation, however. First, if AZ were able to pass the plasma membrane of *Lingulodinium*, this would support instead a role for internal CA isoforms in carbon acquisition. However, AZ is often used as a membrane-impermeable CA inhibitor for phytoplankton (Elzenga et al., 2000; Tortell and Morel, 2002; Morant-Manceau et al., 2007), suggesting any effect on internal CA activity may be small. We also note that our measured cell surface CA activity is almost completely abolished by AZ (Fig. 3C), indicating that any effect of AZ must take this into account. Second, it is possible that pH changes might have independent effects on the cells other than the rapid change in  $[\text{CO}_2]$ . For example, it has been reported that the pH can directly affect growth of dinoflagellates in a manner virtually independent of the effect on inorganic carbon (Hansen et al., 2007). However, these studies used algae grown for extended periods at different pHs, whereas our assays take place over only 30 min, unlikely to be sufficient time for significant physiological acclimation to a new pH. Furthermore, in our brief  $^{14}\text{C}$  uptake assays varying DIC at three different pHs (Fig. 4), carbon fixation rates at all pHs clearly aligned on an axis of calculated  $[\text{CO}_2]$ . Thus, while we cannot exclude the possibility that photosynthetic parameters may change as a complex function of pH and DIC, it seems more reasonable to assume that it is the  $[\text{CO}_2]$ , as calculated from known chemical equations and rate constants, that constrains photosynthetic rate and that direct effects of pH are negligible.

A theoretical underpinning of carbon limitation by the rate of diffusion in aqueous solution has been previously proposed for diatoms that do not possess a CCM (Riebesell et al., 1993; Wolf-Gladrow and Riebesell, 1997). Our results suggest that the  $\delta$ -CA may be the catalyst that fulfills this role in *L. polyedrum*. Strikingly, the proportional inhibition of photosynthesis by AZ is more marked at intermediate concentrations of  $\text{CO}_2$ , an observation recapitulated by the calculated  $[\text{CO}_2]$  at the cell boundary (Fig. 5D). At high  $\text{CO}_2$  concentrations, inhibition of eCA had less effect than at intermediate concentrations of  $\text{CO}_2$  because even a substantial demand for carbon is unable to reduce  $\text{CO}_2$  below saturating levels. At the other end of the  $[\text{CO}_2]$  spectrum, internal recycling of respired  $\text{CO}_2$  or pho-

torespiration could become proportionately more important, causing an underestimate in photosynthetic rate as measured by uptake of  $^{14}\text{C}$  from the external medium. In this case, the demand for external  $\text{CO}_2$  would be lower than expected, resulting in a proportionately smaller decrease in cell surface  $[\text{CO}_2]$  and proportionately smaller effect of eCA inhibition. Taken together, these results suggest not only that *L. polyedrum* uses  $\text{CO}_2$  preferentially, as do several other dinoflagellates (Colman et al., 2002), but also that the external  $\delta$ -CA may have a role in providing this  $\text{CO}_2$ .

The observation that  $\text{CO}_2$  diffusion rates can limit photosynthesis in diatoms (Riebesell et al., 1993) initially seems at odds with the fact that the diatom  $\delta$ -CA is not localized to the plasma membrane. However, there may well be other plasma membrane CAs in these organisms. Indeed, CA immunoreactivity has been observed over the cell membrane space in air-grown *Phaeodactylum* (Szabo and Colman, 2007). It has also been proposed that the acidic silica cell wall around diatoms may serve as a buffer to make conversion of  $\text{HCO}_3^-$  to  $\text{CO}_2$  more efficient (Milligan and Morel, 2002). To date, the only characterized CA is from *Phaeodactylum tricornutum*, a  $\beta$ -CA called PtCA1 (Satoh et al., 2001) localized in the chloroplast stroma adjacent to the thylakoid membrane (Tanaka et al., 2005). Inhibition by the membrane-permeable CA inhibitor EZA was observed to increase the half-saturation constant ( $K_m$ ) for photosynthesis (Satoh et al., 2001), although it cannot be concluded that this is the only target for the inhibitor.

It must be emphasized that the results reported here consider photosynthetic rate as a function of  $\text{CO}_2$  concentration at the cell surface. We know neither the form nor the concentration of DIC within the cytoplasm, yet clearly, in the absence of active transport, uptake of  $\text{CO}_2$  would require a concentration gradient between the external medium and Rubisco. It would be interesting to determine internal  $\text{CO}_2$  concentrations to assess the possibility of active transport. It would also be of interest to trace the movement of  $\text{CO}_2$  to the plastid following its entry into the cell.

We do not yet know whether the plasma membrane  $\delta$ -CA described here will be a conserved feature of dinoflagellate carbon acquisition. EST sequences indicate the presence of a  $\delta$ -CA in *Alexandrium*, *Karlodinium*, and *Karenia*, but *Amphidinium* has no immunoreactivity with the  $\delta$ -CA antibody and no  $\delta$ -CA ESTs can be identified from this species. Furthermore, physiological demonstrations of external CA in dinoflagellates are few and often contradictory. For example, different reports using *Prorocentrum minimum* suggest that it either has an external CA (Nimer et al., 1997) or lacks an external CA and uses  $\text{HCO}_3^-$  directly (Rost et al., 2006). The situation for *A. carterae* is similar, with some reports describing the presence (Nimer et al., 1997) and others the absence (Dason et al., 2004) of external CA activity. Some of these differences in external CA activities may reflect leakage of internal CA during the measurements because some dinoflagellates may be

less robust than the *Lingulodinium* used here. Alternatively, the difference may reflect different environmental conditions under which the cells were grown or the use of different isolates. Clearly, the identification of a  $\delta$ -CA in dinoflagellates will provide important new tools to address these issues.

## MATERIALS AND METHODS

### Cell Culture Conditions

*Lingulodinium polyedrum* (CCMP 1936; formerly *Gonyaulax polyedra*) was obtained from the Provasoli-Guillard Culture Center for Marine Phytoplankton (Boothbay Harbor, Maine) and cultured as described (Wang et al., 2005a). Cultures were grown in *f*/2 medium under 12 h light ( $40 \mu\text{mol m}^{-2} \text{s}^{-1}$  cool-white fluorescent light) and 12 h dark at a temperature of  $18^\circ\text{C} \pm 1^\circ\text{C}$ , and experimental samples were taken from late-log-phase cultures (approximately  $0.5 \mu\text{mol Chl } a/\text{mL}$ ) midway through the light phase. Total DIC ranged between 1.8 and 2.1 mmol/L as measured with a  $\text{CO}_2$  ISE electrode (Analytical Sensors), and total alkalinity was approximately 2.1 mEq/L as measured by acid titration, conditions that resemble those found in very dense coastal algal blooms (Hansen et al., 2007). Culture pH ranged daily between pH 8.4 and 8.9 as previously described (Eisensamer and Roenneberg, 2004).

### Photosynthetic Carbon Fixation Measurements

Rates of photosynthetic carbon fixation were determined by  $^{14}\text{C}$  incorporation into acid-insoluble material. For the assays, duplicate 1-mL samples were taken for cell counts and 70-mL samples of late-log-phase culture were removed to a darkened room.  $\text{NaH}^{14}\text{CO}_3(\text{aq})$  (ICN; 310 MBq/mmol) was added to bring the 70-mL culture sample (pH approximately 8.7, DIC = 2.0 mM, total alkalinity 2.1 mEq/L) to a specific activity of 1.1 kBq/mmol. This  $^{14}\text{C}$ -enriched culture was gently distributed in 940- $\mu\text{L}$  aliquots into wells of duplicate microtiter plates preloaded with 50  $\mu\text{L}$  of 1 M Tris buffer (pH 8, 8.5, 8.7, 8.9, 9.2, or 9.5) and either 10  $\mu\text{L}$  of dimethyl sulfoxide (DMSO) or 10  $\mu\text{L}$  of 100 mM AZ in DMSO (final concentration 1 mM). The final pH in the microtiter samples was measured with unlabeled cultures and found to range between pH 8.05 and pH 9.44. The  $[\text{CO}_2]$  concentrations at the different pH values were calculated according to Schulz et al. (2006) and were not corrected for the slight changes to DIC caused by addition of the different pH buffers. DIC cannot be measured in Tris buffers, but if buffer stocks were at their maximal air-equilibrium values, the final  $[\text{CO}_2]$  would differ by a maximum of  $0.5 \mu\text{mol/L}$  (at pH 9.5). The interconversion of  $\text{HCO}_3^-$  and  $\text{CO}_2$  is reported to be measured on a time scale of tens of seconds (Schulz et al., 2006), so prepared microtiter plates were loaded, sealed from the atmosphere, and then held in the dark for 5 min to allow equilibration of  $\text{HCO}_3^-$  and  $\text{CO}_2$  at the new pH. The  $\text{CO}_2$  concentrations were also uncorrected for  $\text{CO}_2$  present in the sealed airspace (this approximately 1-mL volume would contribute  $<1\%$  to the DIC pool in the samples) or produced by respiration (based on the amount of available DIC is fixed and assuming equal rates of respiration, we estimate  $<2\%$  contamination of external DIC from respiratory  $\text{CO}_2$ ).

One plate from each duplicate pair was exposed to the light under culture conditions for 30 min, while the other was kept in the dark to quantify the small, but significant, nonphotosynthetic  $^{14}\text{C}$  fixation (roughly 10% of light fixation). During the incubation in the light, between 0.2% and 1.9% of available DIC was fixed, and the carbon fixation rates were approximately linear over the 10- to 30-min range. For each experimental condition, the reaction in quadruplicate samples was halted by the addition of 0.2 volumes each of 5 M HCl and methanol to stop uptake and drive off excess inorganic  $\text{H}^{14}\text{CO}_3^-$ . Additional samples were stopped with 5 M NaOH to trap all inorganic  $\text{H}^{14}\text{CO}_3^-$  to confirm that the specific radioactivity was maintained throughout the incubation. Excess  $^{14}\text{C}$  in the acidified samples was allowed to escape from the unsealed plates overnight, the samples transferred to scintillation vials with 3-mL ScintiVerse cocktail (Fisher Scientific), and the radioactivity measured in a TriCarb 2800TR scintillation counter (Perkin-Elmer). Photosynthesis rates are reported as light-induced C fixation minus dark C fixation.

For some experiments, cells were concentrated by gentle centrifugation (30 s at 1,000g), then resuspended in artificial seawater (0.46 M NaCl, 0.01 M KCl, 0.01 M  $\text{CaCl}_2$ , 0.05 M  $\text{MgCl}_2$ ) containing known amounts of DIC as the

only electron sink. These concentrated cultures were treated as above. However, whereas this protocol allows the culture medium to be replaced with medium of differing DIC concentrations, centrifugation causes the flagella to break, and cells rapidly sink to the bottom of the ELISA plate wells.

Last, in experiments varying DIC, the addition of 10 or 30 mM  $\text{HCO}_3^-$  to artificial seawater decreased the pH of despite the buffering action of the 50 mM Tris. For these samples, the pH measured in a separate aliquot of buffered artificial seawater containing the DIC was used to calculate  $\text{CO}_2$  concentrations.

### cDNA Cloning and Screening

PCR fragments were amplified using DNA derived from a previously constructed cDNA library using degenerate primers prepared from conserved regions in sequence alignments of  $\alpha$ -,  $\beta$ -, and  $\gamma$ -CA family members. The primer pair (5'-ATGSARAARATGATG-3' and 5'-CCNGTRCTNCGNAC-RCC-3') amplified a 304-bp fragment with significant homology to  $\delta$ -CA from the diatom *Thalassiosira weissflogii*. This fragment was used as a probe to isolate longer clones from the library by colony hybridization. Eight sequences were recovered, and could be put into two groups termed LpCA1 and LpCA2 whose sequences were 80% identical (85% similar) at the amino acid level and shared between 58% and 62% sequence identity with a  $\delta$ -CA from the diatom *Thalassiosira*. Although the cDNA sequences were incomplete (approximately 1.1 and 1.2 kb, respectively), the full 5' sequence of LpCA2 was recovered by PCR using an oligonucleotide containing the sequence of the trans-splice leader (5'-CCGTAGCCATTTGGCTCAAG-3') found in all dinoflagellate mRNA (Zhang et al., 2007). LpCA1 and a complete 1.6-kb LpCA2 sequence were deposited in GenBank under accession numbers EU044833 and EU044834. Most sequence analysis, including phylogenetic reconstruction, was performed using MacVector software (Accelrys) using the CA sequence from the diatom *T. weissflogii* (AAV39532), the C-terminal end of a CA from the haptophyte *Emiliania huxleyi* (ABG37687), and CA sequences assembled from ESTs for the chlorophyte *Micromonas* (EC848383 and EC847708) and the haptophyte *Isochrysis galbana* (EC146202 and EC142695). The possible presence of a signal peptide was tested with SignalP (<http://www.cbs.dtu.dk/services/SignalP>), the presence of palmitoylation sites was checked with CSS-Palm ([http://bioinformatics.lcd-ustc.org/css\\_palm](http://bioinformatics.lcd-ustc.org/css_palm)), and the predicted sequence topology of the complete LpCA2 protein was evaluated using Phobius (<http://phobius.cgb.ki.se>).

### Antibody Purification and Electrophoretic Analyses

Antibody raised against the  $\delta$ -CA of *Thalassiosira* (Roberts et al., 1997) was generously provided by F.M.M. Morel (Princeton University). The antibody was affinity purified using the LpCA2 cDNA expressed in bacteria and transferred to nitrocellulose after SDS-PAGE (Claeysen et al., 2006). For electrophoretic analyses on standard SDS-PAGE, protein samples were boiled for 5 min in five packed cell volumes 2% SDS, 0.7 mM  $\beta$ -mercaptoethanol, 62.5 mM Tris-HCl, pH 6.8, and 10% glycerol and electrophoresed at 150 V on 12% SDS-PAGE. For 2D-PAGE, proteins were precipitated with 3 volumes of chloroform-methanol and the pellets dried and resuspended in 265  $\mu\text{L}$  of 8 M urea, 4% CHAPS, 20 mM dithiothreitol, and 0.5% pH 3 to 10 nonlinear (NL) immobilized pH gradient (IPG) buffer. This sample was used to rehydrate a 13-cm IPG strip, pH 3 to 10 NL, and was electrophoresed using an IPGphor isoelectric focusing system (GE Healthcare) for 20,000 Vh. For the second dimension, strips were incubated 20 min in SDS equilibration buffer (50 mM Tris-HCl, pH 8.8, 6 M urea, 30% glycerol, and 2% SDS) and then run on a 12% SDS-PAGE. For immunoblotting, proteins were transferred electrophoretically to polyvinylidene difluoride membranes for 20 min at 20 V using a semidry transfer cell (Bio-Rad) and stained with Ponceau red to confirm transfer. Membranes were blocked for 10 min in Tris-buffered saline plus Tween (5 mM Tris-HCl, pH 8.0, 137 mM NaCl, 2.5 mM KCl, and 0.05% Tween 20) containing 3% bovine serum albumin and incubated with antibodies overnight at  $4^\circ\text{C}$  diluted in fresh buffer.

Cell surface proteins were iodinated with  $\text{Na}^{125}\text{I}$  as described (Bertomeu et al., 2003), except that the purified cell wall fractions were extracted with SDS sample buffer and precipitated with 3 volumes of chloroform-methanol before resuspension in sample buffer for 2D gels.

### Immunocytochemistry

Cells were harvested from the culture by centrifugation, washed with 0.4 M phosphate-buffered saline (PBS), and fixed with 3% glutaraldehyde in 0.4 M PBS for 30 min without osmium to preserve antigenicity on the sections. The

fixed cells were washed three times in PBS and water, dehydrated with a standard ethanol series, and embedded in LR White resin polymerized for 24 h at 60°C in gelatin capsules. Thin sections were cut for transmission electron microscopy, poststained with uranyl acetate, and observed using a JEOL JEM 100S microscope operating at 80 kV. Immunolabeling with affinity-purified anti- $\delta$ -CA was performed essentially as described (Nassoury et al., 2001) using 1/100 dilution of the primary antibody and a 1/100 dilution of 20 nm gold labeled anti-rabbit IgG (Ted Pella) as a secondary antibody. No labeling of the cell sections was observed with the secondary antibody alone.

## CA Assays

CA activity was assayed in whole cells by an electrometric method similar to Wilbur and Anderson (1948). Culture samples containing approximately  $10^5$  cells were pelleted by gentle centrifugation (<10 s) in an ICN clinical centrifuge and resuspended in 2.7 mL of CA assay buffer (300 mM sorbitol, 1 mM  $\text{MgCl}_2 \cdot 6\text{H}_2\text{O}$ , 20 mM Tris, pH 8.8, at 0°C) on ice. The pH of the assay was logged by computer (PH-BTA pH sensor; Vernier Software & Technology) after addition of 0.9 mL of  $\text{CO}_2$ -saturated water. The buffer was agitated by a magnetic stir-bar at the slowest rate possible to maintain accurate pH measurement, and, at this rate, cell breakage as determined by microscopic examination was below 1% even for bouts of stirring much longer than the 1 or 2 min required for the assay. After addition of  $\text{CO}_2$ -saturated water, pH of the assay buffer fell rapidly because of  $\text{H}^+$  liberated by the hydration of  $\text{CO}_2$ . The times elapsed over intervals of particular pH levels were converted into absolute rates of  $\text{CO}_2$  hydration to  $\text{HCO}_3^-$  by acid titration of the CA assay buffer to these pH levels in a method similar to Ratti et al. (2007). Absolute rates of spontaneous  $\text{CO}_2$  hydration were used as controls and determined by addition of 0.9 mL of  $\text{CO}_2$ -saturated water to buffer alone, without intact cells or extracts. Activity attributable to cell surface CA was determined by subtracting the spontaneous rates from the faster rates of  $\text{CO}_2$  hydration in samples containing intact cells and was confirmed to be due to CA by addition of the CA inhibitor AZ (1 mM), which rapidly reduced the  $\text{CO}_2$  hydration rate to control levels.

For determining CA activity in cell extracts, cells were pelleted in a clinical centrifuge, resuspended in CA assay buffer with 1% Saponin (practical grade; ICN), and broken in a Wheaton glass homogenizer on ice. The homogenate was fractionated into a soluble supernatant and insoluble pellet fraction by centrifugation for 2 min at 12,000g in an Eppendorf centrifuge (5415D). Each fraction was then diluted to 2.7 mL in CA assay buffer and processed through the protocol as for whole cells above. The activity in each crude fraction would decline over time; thus, only one fraction was processed from alternate cell samples and the other fraction discarded to avoid bias due to the time required to assay the activity of each fraction.

## Carbon Limitation Calculations

The  $[\text{CO}_2]$  as a function of the distance from the cell center ( $r$ ) was calculated from the rate of photosynthesis ( $Q_a$ , in  $\mu\text{mol CO}_2$  fixed per cell per second) using the following equation:

$$[\text{CO}_2]_r = [\text{CO}_2]_{\text{eq}} - \frac{1,000 \times Q_a}{4\pi \times r D_{\text{CO}_2} \left(1 + \frac{a}{a_k}\right)} e^{\left(\frac{a-r}{a_k}\right)} \quad (1)$$

with  $D_{\text{CO}_2}$  the diffusion constant for  $\text{CO}_2$  ( $1.5 \times 10^{-5} \text{ cm}^2/\text{s}$ ),  $a$  the radius of the cell (0.0017 cm; Nassoury et al., 2001), and  $a_k$  the reacto-diffusive length (Riebesell et al., 1993). A unit conversion factor of 1,000  $\text{cm}^3/\text{L}$  is included to allow use of concentrations in  $\mu\text{M}$ . The equilibrium  $\text{CO}_2$  concentrations in seawater were calculated based on pH and titrated alkalinity measurements using the formula:

$$[\text{CO}_2]_{\text{eq}} = \frac{(k_{-1}[\text{H}^+] + 1k_{-4})}{(k_{+1} + k_{+4}[\text{OH}^-])} \quad (2)$$

using the rate constants  $k_{+1} = 3.7 \times 10^{-2} \text{ s}^{-1}$ ;  $k_{-1} = 2.67 \times 10^4 \text{ kg mol}^{-1} \text{ s}^{-1}$ ;  $k_{+4} = 2.23 \times 10^3 \text{ kg mol}^{-1} \text{ s}^{-1}$ ; and  $k_{-4} = 9.7 \times 10^{-5} \text{ s}^{-1}$  as described (Schulz et al., 2006).

Sequence data from this article can be found in the GenBank/EMBL data libraries under accession numbers EU044833 and EU044834.

## Supplemental Data

The following materials are available in the online version of this article.

**Supplemental Alignment Data S1.** Sequence alignment of LpCA1 and LpCA2 with the diatom TWCA.

## ACKNOWLEDGMENTS

We thank Dr. Haewon Park and Dr. François M.M. Morel (Princeton University) for generously providing anti- $\delta$ -CA raised against the diatom enzyme. We also thank L. Pelletier (Université de Montréal) for technical assistance with the electron microscope.

Received January 29, 2008; accepted April 18, 2008; published May 8, 2008.

## LITERATURE CITED

- Behrenfeld MJ, O'Malley RT, Siegel DA, McClain CR, Sarmiento JL, Feldman GC, Milligan AJ, Falkowski PG, Letelier RM, Boss ES (2006) Climate-driven trends in contemporary ocean productivity. *Nature* **444**: 752–755
- Berman-Frank I, Kaplan A, Zohary T, Dubinsky Z (1995) Carbonic anhydrase activity in the bloom forming dinoflagellate *Peridinium gatunense*. *J Phycol* **31**: 906–913
- Berman-Frank I, Zohary T, Erez J, Dubinsky Z (1994)  $\text{CO}_2$  availability, carbonic anhydrase, and the annual dinoflagellate bloom in Lake Kinneret. *Limnol Oceanogr* **39**: 1822–1834
- Bertomeu T, Hastings JW, Morse D (2003) Vectorial labeling of dinoflagellate cell surface proteins. *J Phycol* **39**: 1254–1260
- Claeysen E, Wally O, Matton DP, Morse D, Rivoal J (2006) Cloning, expression, purification, and properties of a putative plasma membrane hexokinase from *Solanum chacoense*. *Protein Expr Purif* **47**: 329–339
- Colman B, Huertas IE, Bhatti S, Dason JS (2002) The diversity of inorganic carbon acquisition mechanisms in eukaryotic microalgae. *Funct Plant Biol* **29**: 261–270
- Dason JS, Huertas IE, Colman B (2004) Source of inorganic carbon for photosynthesis in two marine dinoflagellates. *J Phycol* **40**: 285–292
- Eisensamer B, Roenneberg T (2004) Extracellular pH is under circadian control in *Gonyaulax polyedra* and forms a metabolic feedback loop. *Chronobiol Int* **21**: 27–41
- Elzenga JTM, Prins HBA, Stefels J (2000) The role of extracellular carbonic anhydrase activity in inorganic carbon utilization of *Phaeocystis globosa* (Prymnesiophyceae): a comparison with other marine algae using the isotopic disequilibrium technique. *Limnol Oceanogr* **45**: 372–380
- Fagan T, Hastings JW, Morse D (1998) The phylogeny of glyceraldehyde-3-phosphate dehydrogenase indicates lateral gene transfer from cryptomonads to dinoflagellates. *J Mol Evol* **47**: 633–639
- Giordano M, Beardall J, Raven JA (2005)  $\text{CO}_2$  concentrating mechanisms in algae: mechanisms, environmental modulation, and evolution. *Annu Rev Plant Biol* **56**: 99–131
- Hansen PJ, Lundholm N, Rost B (2007) Growth limitation in marine red-tide dinoflagellates: effects of pH versus inorganic availability. *Mar Ecol Prog Ser* **334**: 63–71
- Harper JT, Waanders E, Keeling PJ (2005) On the monophyly of chromalveolates using a six-protein phylogeny of eukaryotes. *Int J Syst Evol Microbiol* **55**: 487–496
- Jacobson BS, Fong F, Heath RL (1975) Carbonic anhydrase of spinach: studies on its location, inhibition, and physiological function. *Plant Physiol* **55**: 468–474
- Keeling PJ, Inagaki Y (2004) A class of eukaryotic GTPase with a punctate distribution suggesting multiple functional replacements of translation elongation factor 1alpha. *Proc Natl Acad Sci USA* **101**: 15380–15385
- Lane TW, Morel FM (2000) Regulation of carbonic anhydrase expression by zinc, cobalt, and carbon dioxide in the marine diatom *Thalassiosira weissflogii*. *Plant Physiol* **123**: 345–352
- Lane TW, Saito MA, George GN, Pickering IJ, Prince RC, Morel FM (2005) Biochemistry: a cadmium enzyme from a marine diatom. *Nature* **435**: 42
- Leggat W, Badger MR, Yellowlees D (1999) Evidence for an inorganic carbon-concentrating mechanism in the symbiotic dinoflagellate *Symbiodinium*. *Plant Physiol* **121**: 1247–1255
- Leggat W, Marendy EM, Baillie B, Whitney SM, Ludwig M, Badger MR, Yellowlees D (2002) Dinoflagellate symbioses: strategies and adapta-

- tions for the acquisition and fixation of inorganic carbon. *Funct Plant Biol* **29**: 309–322
- Milligan AJ, Morel FM** (2002) A proton buffering role for silica in diatoms. *Science* **297**: 1848–1850
- Morant-Manceau A, Nguyen TLN, Pradier E, Tremblin G** (2007) Carbonic anhydrase activity and photosynthesis in marine diatoms. *Eur J Phycol* **42**: 263–270
- Moroney JV, Bartlett SG, Samuelsson G** (2001) Carbonic anhydrases in plants and algae. *Plant Cell Environ* **24**: 141–153
- Moroney JV, Husic HD, Tolbert NE** (1985) Effect of carbonic anhydrase inhibitors on inorganic carbon accumulation by *Chlamydomonas reinhardtii*. *Plant Physiol* **79**: 177–183
- Morse D, Salois P, Markovic P, Hastings JW** (1995) A nuclear encoded form II RuBisCO in dinoflagellates. *Science* **268**: 1622–1624
- Nassoury N, Fritz L, Morse D** (2001) Circadian changes in ribulose-1,5-bisphosphate carboxylase/oxygenase distribution inside individual chloroplasts can account for the rhythm in dinoflagellate carbon fixation. *Plant Cell* **13**: 923–934
- Nimer NA, Brownlee C, Merrett MJ** (1999) Extracellular carbonic anhydrase facilitates carbon dioxide availability for photosynthesis in the marine dinoflagellate *Prorocentrum micans*. *Plant Physiol* **120**: 105–112
- Nimer NA, Iglesias-Rodriguez MD, Merrett MJ** (1997) Bicarbonate utilization by marine phytoplankton species. *J Phycol* **33**: 625–631
- Ratti S, Morse D, Giordano M** (2007) CO<sub>2</sub> concentrating mechanisms of the potentially toxic dinoflagellate *Protoceratium reticulatum*. *J Phycol* **43**: 693–701
- Raven JA** (1997) CO<sub>2</sub>-concentrating mechanism: a direct role for thylakoid lumen acidification? *Plant Cell Environ* **20**: 147–154
- Riebesell U, Wolf-Gladrow DA, Smetacek V** (1993) Carbon dioxide limitation of marine phytoplankton growth rates. *Nature* **361**: 249–251
- Roberts SB, Lane TW, Morel FMM** (1997) Carbonic anhydrase in the marine diatom *Thalassiosira weissflogii* (Bacillariophyceae). *J Phycol* **33**: 845–850
- Rost B, Richter KU, Riebesell U, Hansen PJ** (2006) Inorganic carbon acquisition in red tide dinoflagellates. *Plant Cell Environ* **29**: 810–822
- Rumeau D, Cuiné S, Fina L, Gault N, Nicole M, Peltier G** (1996) Subcellular distribution of carbonic anhydrase in *Solanum tuberosum* L. leaves. *Planta* **199**: 79–88
- Satoh D, Hiraoka Y, Colman B, Matsuda Y** (2001) Physiological and molecular biological characterization of intracellular carbonic anhydrase from the marine diatom *Phaeodactylum tricorutum*. *Plant Physiol* **126**: 1459–1470
- Schulz KG, Riebesell U, Rost B, Thoms S, Zeebe RE** (2006) Determination of the rate constants for the carbon dioxide to bicarbonate inter-conversion in pH buffered seawater systems. *Mar Chem* **100**: 53–65
- So AK, Espie GS, Williams EB, Shively JM, Heinhorst S, Cannon GC** (2004) A novel evolutionary lineage of carbonic anhydrase (epsilon class) is a component of the carboxysome shell. *J Bacteriol* **186**: 623–630
- Soto AR, Zheng H, Shoemaker D, Rodriguez J, Read BA, Wahlund TM** (2006) Identification and preliminary characterization of two cDNAs encoding unique carbonic anhydrases from the marine alga *Emiliania huxleyi*. *Appl Environ Microbiol* **72**: 5500–5511
- Spalding MH** (2008) Microalgal carbon-dioxide-concentrating mechanisms: *Chlamydomonas* inorganic carbon transporters. *J Exp Bot* **59**: 1463–1473
- Sültemeyer D** (1998) Carbonic anhydrase in eukaryotic algae: characterization, regulation and possible function during photosynthesis. *Can J Bot* **76**: 962–972
- Szabo E, Colman B** (2007) Isolation and characterization of carbonic anhydrases from the marine diatom *Phaeodactylum tricorutum*. *Physiol Plant* **129**: 484–492
- Tanaka Y, Nakatsuma D, Harada H, Ishida M, Matsuda Y** (2005) Localization of soluble beta-carbonic anhydrase in the marine diatom *Phaeodactylum tricorutum*. Sorting to the chloroplast and cluster formation on the girdle lamellae. *Plant Physiol* **138**: 207–217
- Tortell PD, Morel FM** (2002) Sources of inorganic carbon for phytoplankton in the eastern Subtropical and Equatorial Pacific Ocean. *Limnol Oceanogr* **47**: 1012–1022
- Tripp BC, Smith K, Ferry JG** (2001) Carbonic anhydrase: new insights for an ancient enzyme. *J Biol Chem* **276**: 48615–48618
- Van K, Spalding MH** (1999) Periplasmic carbonic anhydrase structural gene (*Cah1*) mutant in *Chlamydomonas reinhardtii*. *Plant Physiol* **120**: 757–764
- Waller RF, Slamovits CH, Keeling PJ** (2006) Lateral gene transfer of a multigene region from cyanobacteria to dinoflagellates resulting in a novel plastid-targeted fusion protein. *Mol Biol Evol* **23**: 1437–1443
- Wang Y, Jensen L, Hojrup P, Morse D** (2005a) Synthesis and degradation of dinoflagellate plastid-encoded psbA proteins are light-regulated, not circadian-regulated. *Proc Natl Acad Sci USA* **102**: 2844–2849
- Wang Y, MacKenzie T, Morse D** (2005b) Purification of plastids from the dinoflagellate *Lingulodinium*. *Mar Biotechnol* (NY) **7**: 659–668
- Whitney S, Andrews T** (1998) The CO<sub>2</sub>/O<sub>2</sub> specificity of single-subunit ribulose-bisphosphate carboxylase from the dinoflagellate *Amphidinium carterae*. *Aust J Plant Physiol* **25**: 131–138
- Wilbur KM, Anderson NG** (1948) Electrometric and colorimetric determination of carbonic anhydrase. *J Biol Chem* **176**: 147–154
- Williams TG, Colman B** (1996) The effects of pH and dissolved inorganic carbon on external carbonic anhydrase activity in *Chlorella saccharophila*. *Plant Cell Environ* **19**: 485–489
- Williams TG, Turpin DH** (1987) The role of external carbonic anhydrase in inorganic carbon acquisition by *Chlamydomonas reinhardtii* at alkaline pH. *Plant Physiol* **83**: 92–96
- Wolf-Gladrow D, Riebesell U** (1997) Diffusion and reactions in the vicinity of plankton: a refined model for inorganic carbon transport. *Mar Chem* **59**: 17–34
- Zeebe RE, Wolf-Gladrow D, Hansen PJ** (1999) On the time required to establish chemical and isotopic equilibrium in the carbon dioxide system in seawater. *Mar Chem* **64**: 135–153
- Zhang H, Hou Y, Miranda L, Campbell DA, Sturm NR, Gaasterland T, Lin S** (2007) Spliced leader RNA trans-splicing in dinoflagellates. *Proc Natl Acad Sci USA* **104**: 4618–4623